Check for updates

Wiley
International Journal of Energy Research
Volume 2025, Article ID 2329142, 13 pages
https://doi.org/10.1155/er/2329142

WILEY

Research Article

A Shortcut Modeling Platform for Optimizing Catalyst Distribution of the CO_2-to-Methanol Process

Hee Won Lee,[1,2] Kyeongsu Kim,[1,2] Jonggeol Na,[3,4,5] Honggon Kim,[1] Hyunjoo Lee,[1,2] Changsoo Kim,[1,2] Kwang-Deog Jung,[1,2] Won Da Hye,[1,2] KyungJae Tak,[6] and Ung Lee[1,2,7]

[1]*Clean Energy Research Center, Korea Institute of Science and Technology, Seoul 02792, Republic of Korea*
[2]*Division of Energy and Environment Technology, KIST School, Korea University of Science and Technology, Seoul 02792, Republic of Korea*
[3]*Department of Chemical Engineering and Materials Science, Ewha Womans University, Seoul 03760, Republic of Korea*
[4]*Institute for Multiscale Matter and Systems (IMMS), Ewha Womans University, Seoul 03760, Republic of Korea*
[5]*Graduate Program in System Health Science and Engineering, Ewha Womans University, Seoul 03760, Republic of Korea*
[6]*Department of Chemical Engineering, Dankook University, Gyeonggi-do 16890, Republic of Korea*
[7]*Green School, Korea University, Seoul 02841, Republic of Korea*

Correspondence should be addressed to KyungJae Tak; kjtak@dankook.ac.kr and Ung Lee; ulee@kist.re.kr

Received 18 May 2025; Revised 17 November 2025; Accepted 18 November 2025

Academic Editor: Mohammadmahdi Abdollahzadehsangroudi

Copyright © 2025 Hee Won Lee et al. International Journal of Energy Research published by John Wiley & Sons Ltd. This is an open access article under the terms of the Creative Commons Attribution License, which permits use, distribution and reproduction in any medium, provided the original work is properly cited.

Methanol synthesis via CO_2 hydrogenation is increasingly recognized as a pivotal strategy in CO_2 utilization, addressing both environmental concerns and the demand for sustainable chemical production. However, the exothermic nature of methanol synthesis often leads to thermal management issues in reactors, particularly near the inlet. This study proposes an optimized three-stage reactor system with a distinctive approach to catalyst distribution. Each reactor is divided into two zones, culminating in six zones with varied catalyst loadings, specifically designed to alleviate hot spots. The advanced modeling platform developed in this study significantly reduces the computational intensity typically required in such processes. This platform integrates a process simulator with computational fluid dynamics (CFD) modeling, allowing for efficient computation of reaction rates and heat release as well as detailed temperature profiles in both axial and radial directions. Using an efficient Gaussian process Bayesian optimization (GPBO) algorithm, we optimized the catalyst loading with the minimum number of iterations. Our findings indicate a significant decrease in temperature variances in reactors of various sizes: 67.5% in a 2-inch tube reactor, 55.4% in a 1-inch reactor, and 67.3% in a 3/8-inch reactor, when compared to conventional methanol reactor. The maximum temperature differences were notably reduced by up to 15.7 K in the axial direction for 3/8-inch tubes and up to 2.5 K in the radial direction for 2-inch tubes. Additionally, the study provides insights into the promotional effects of CO. This platform not only optimizes reactor performance but also provides a substantial advancement in the computational modeling of methanol synthesis from CO_2.

Keywords: Bayesian optimization; carbon capture and utilization; catalyst loading; CO_2 hydrogenation; computational fluid dynamics; methanol production; reactor design

1. Introduction

Methanol is a versatile chemical, serving as an environmentally friendly fuel substitute, hydrogen carrier, and feedstock for high-value chemicals [1]. Its large market size and wide applicability have made CO_2 conversion to methanol a key technology in carbon capture and utilization (CCU) [2]. Conventional methanol production largely relies on indirect conversion of natural gas, coal, or biomass into methanol via synthesis gas (syngas). This indirect approach offers high selectivity, low production cost, and high process yield [3]; however, it is energy-intensive and generates substantial CO_2 emissions [3]. Consequently, the direct CO_2 hydrogenation to methanol (CTM) has emerged as an increasingly attractive alternative.

Direct CO_2 hydrogenation is typically conducted under mild conditions (200–300°C, 20–80 bar) and consumes CO_2 as a raw material, providing a more sustainable pathway. Literature reports single-pass CO_2 conversions of 18%–24% [4, 5]. Such low conversion requires oversized reactors and high recycle ratios, increasing both capital and operating costs. Therefore, maximizing CO_2 conversion remains a major research objective. Optimizing conversion within a reactor is challenging due to nonlinear relationships among operating variables and inherent trade-offs; for instance, CO_2 hydrogenation at lower temperature is thermodynamically advantageous but slows kinetics.

Several studies have explored alternative reactor designs to enhance CO_2 conversion [6–8]. Most of these studies, however, focus on case studies or simple sensitivity analyses and do not incorporate optimization algorithms. Cui and Kær [9] compared adiabatic, gas-cooled, and water-cooled reactors for syngas-to-methanol (STM) process and CTM process. They showed that the water-cooled reactor is more advantageous for the CTM process (operated at 220–280°C) because reaction heat on the tube side is efficiently removed by shell-side cooling water. Kiss et al. [10] proposed a multitubular reactor for direct CO_2 hydrogenation, and Lee et al. [11] extended it to a multistage reactor system. However, those studies conducted either computational fluid dynamics (CFD) simulations at several given conditions without optimization or process simulations/optimizations without CFD simulations.

Since CO_2 hydrogenation is exothermic, uneven temperature distribution is common, highlighting the need to manage hot spots and prevent thermal runaway. Temperature maldistribution and hot spot formation have even been reported in industrial-scale methanol reactors, such as Lurgi mega-methanol dual reactors [12, 13]. Rahimpour's group identified flow maldistribution and phase instability in large-scale methanol production [14, 15]. Using CFD, they demonstrated the detrimental effects of maldistribution on reaction performance [16]. CFD simulations are capable of analyzing temperature profiles within a methanol reactor in both 2D and 3D dimensions, specifically in the axial and radial directions. Consequently, they can be used to investigate effects such as internal heat diffusion and to identify locations of hot spot formation. Optimizing reactor design is, therefore, critical not only for safe operation but also for maximizing productivity [17–19]. Hot spots from locally high reaction rates can lead to thermal runaway and catalyst deactivation [20]. Extensive research has aimed to optimize heat distribution, improve product yield, and mitigate catalyst deactivation [21–23]. The efficiency of catalyst utilization can be enhanced by reducing hot spots, thereby extending the lifetime of the catalyst and increasing overall process efficiency. In addition, methanol synthesis can be enhanced by reactions that are conducted at relatively lower temperatures. Nájera et al. [23] proposed a proportional-integral controller with a dynamic setpoint based on the reactor feed temperature, while Montebelli et al. [22]. designed structured reactors with enhanced radial heat transfer efficiency, improving temperature profiles and benefiting small-scale gas-to-liquid and biomass-to-liquid processes. Agrawal et al. [21] developed a 3D two-phase model to study local interphase heat and mass transport, showing that uniform flow can become unstable to small transverse perturbations, causing maldistributed flows and localized hot spots. Mitigation strategies include diluting reactant concentrations, limiting conversion levels, and implementing multistage reactors with intercooling. Unlike heat-transfer approaches, such as reactor modification or intercooling, our focus is on managing reaction heat via uneven catalyst loading along the reactor length—a simpler and scalable strategy that does not require complex modifications or auxiliary cooling systems.

CFD is an effective tool for predicting internal reactor states, particularly where experimental measurements are challenging. CFD modeling is widely used in complex reactors, such as microchannel, monolith, and multitubular reactors, relevant to processes, including methanol-to-hydrogen conversion, methane reforming, electrochemical CO_2 conversion [24–26], and Fischer-Tropsch synthesis [27–30]. For instance, Sari and Sabziani [27] used CFD to model methanol steam reforming in a microchannel reactor, confirming that both mixture-averaged and Maxwell–Stefan diffusion models closely matched experimental data. CFD can also model monolith reactors with Langmuir–Hinshelwood kinetics and packed-bed reactors with comprehensive process models [31, 32].

From a temperature-control perspective, CFD provides insights for both exothermic and endothermic reactions [29]. Studies have used 2D and 3D CFD to investigate temperature distribution and heat transfer in fixed-bed reactors [33–35]. Zhu et al. [36] analyzed temperature differences between the center and wall in a nonadiabatic multitubular reactor, while Son et al. [37] demonstrated improved thermal control in a bayonet-type fixed-bed reactor by introducing cool feed gas to the inner tube and coolant to the outer tube, with the catalyst layer in the middle tube. CFD can also be applied to direct CO_2 hydrogenation reactors, providing detailed internal temperature, pressure, and flow profiles that support reactor design and operation with consideration of reaction heat effects. Nevertheless, CFD-based design poses significant computational challenges due to large, nonconvex systems of equations and the complex interplay of variables [38]. The intricate interplay of variables and parameters in reactor systems further complicates the process, necessitating advanced computational approaches for accurate modeling and simulation.

Herein, we present a novel optimization platform for a multistage, multitubular reactor system for methanol production via direct CO_2 hydrogenation. Central to our strategy is uneven catalyst loading to achieve uniform temperature distribution. The system consists of a three-stage reactor, each divided into two parts, yielding six distinct catalyst loading zones. These loadings were systematically optimized using Gaussian process Bayesian optimization (GPBO) [11, 39, 40]. CFD simulations were conducted at each optimization iteration to evaluate precise temperature profiles. We also investigated the impact of reactor tube sizes (2-, 1-, and 3/8-inch

ijer, 2025, 1, Downloaded from https://onlinelibrary.wiley.com/doi/10.1155/er/2329142 by Ewha Womans University Library, Wiley Online Library on [20/05/2026]. See the Terms and Conditions (https://onlinelibrary.wiley.com/terms-and-conditions) on Wiley Online Library for rules of use; OA articles are governed by the applicable Creative Commons License

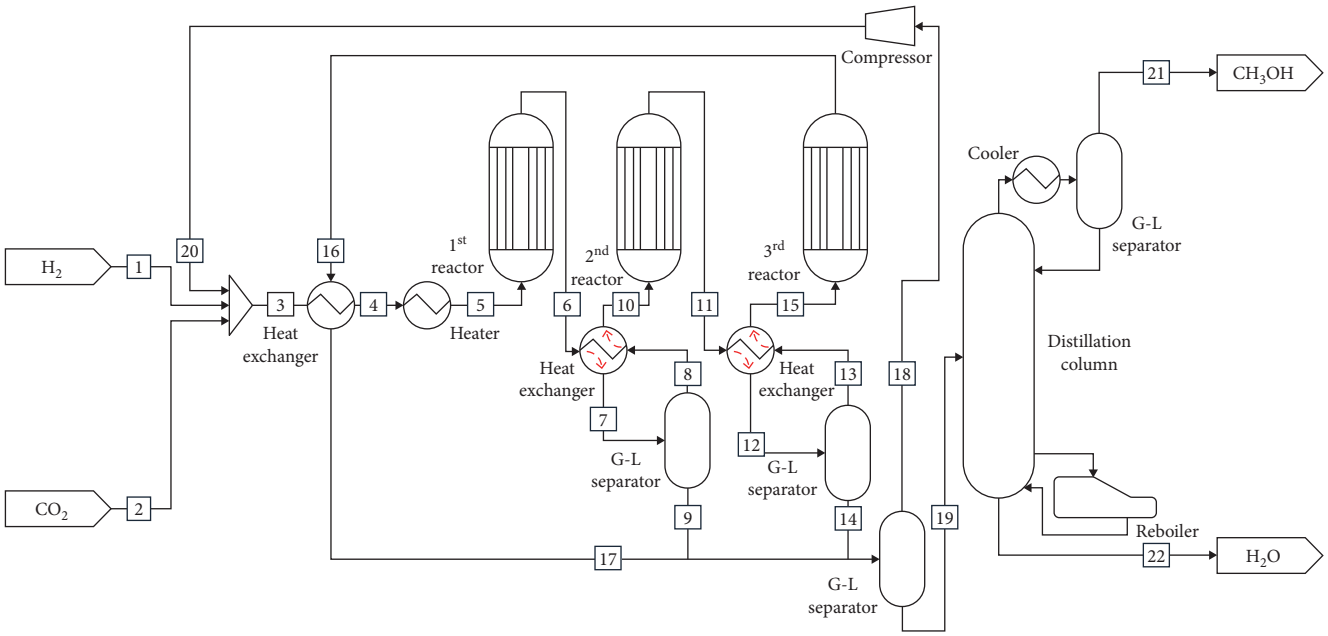


FIGURE 1: Schematic of the three-stage reactor system for methanol production. The system consists of three shell-and-tube reactors in series, each with two catalyst loading zones, totaling six reaction zones.

tubes) on optimal catalyst distribution and temperature profiles, and compared the results in terms of capital investment, demonstrating the effectiveness of our optimization platform.

2. Model Description

2.1. Direct CO_2 Hydrogenation System for Methanol. Direct CO_2 hydrogenation for methanol production has three major reactions, shown in Equations (1)–(3). The reaction in Equation (1) is the CO_2-to-methanol reaction. However, there is a side reaction in which some amount of CO_2 is converted to CO through a reverse water-gas shift (RWGS) reaction in Equation (2). The by-product CO can also be hydrogenated for methanol synthesis, as expressed in Equation (3). All these reactions occur on the surface of Cu/Zn/Al/Zr catalyst in the reactors.

$$CO_2 + 3H_2 \leftrightarrow CH_3OH + H_2O\,\Delta H_{298K} = -49.16\,\text{kJ/mol}, \quad (1)$$

$$CO_2 + H_2 \leftrightarrow CO + H_2O\,\Delta H_{298K} = 41.21\,\text{kJ/mol}, \quad (2)$$

$$CO + 2H_2 \leftrightarrow CH_3OH\,\Delta H_{298K} = -90.77\,\text{kJ/mol}. \quad (3)$$

The three-stage reactor system for methanol production considered in this study is depicted in Figure 1, which was proposed by Lee et al. [11]. This process has three reactors in series with two catalyst loading zones per reactor, leading to overall six zones. Those reactors are a shell-and-tube type: coolant in the shell side and catalyst in the tube side. To maximize CO_2 conversion, the outlet stream from each reactor is cooled in condensers to separate liquid products (methanol and water), ensuring that only unreacted gases are fed into the next reactor. The reactors use saturated water as the coolant, which absorbs the heat generated by the exothermic reaction with an overall heat transfer coefficient of 1000 $W/m^2/K^1$. Since a significant amount of heat is released at the reactor inlets, the hot water enters at the same temperature as the reactor feeds and flows in the same direction. As it absorbs heat along the reactor length, hot water undergoes partial vaporization, enhancing heat removal efficiency.

TABLE 1: Specification of multitubular reactors in this study.

Parameter	Value
Total length of reactor system (m)	12
Number of reactor stages	3
Number of catalyst loading zones	6
Length of a catalyst loading zone (m)	2
Number of tubes in a reactor	
2-inch tube reactor	810
1-inch tube reactor	3240
3/8-inch tube reactor	23,040

The base case for this study was derived from our previous research, which economically optimized the methanol production process without considering the temperature profile [11]. In that study, 865 kg of Cu/Zn/Al/Zr catalyst produced 12,500 kg of methanol per hour with a purity of 99%. The inlet temperatures of the reactors were 522, 518, and 514 K, respectively. For this study, the same conditions were applied, except for the catalyst loading distribution. While catalyst loadings varied across all six zones, a uniform distribution was assumed within each zone. Additionally, the effect of tube size on the temperature profile was examined. Kiss et al. [10] used 810 tubes with 2-inch tube reactors. Based on this, two other tube types were employed: 3240 tubes with 1-inch reactors and 23,040 tubes with 3/8-inch reactors (Table 1).

ijer, 2025, 1, Downloaded from https://onlinelibrary.wiley.com/doi/10.1155/er/2329142 by Ewha Womans University Library, Wiley Online Library on [20/05/2026]. See the Terms and Conditions (https://onlinelibrary.wiley.com/terms-and-conditions) on Wiley Online Library for rules of use; OA articles are governed by the applicable Creative Commons License

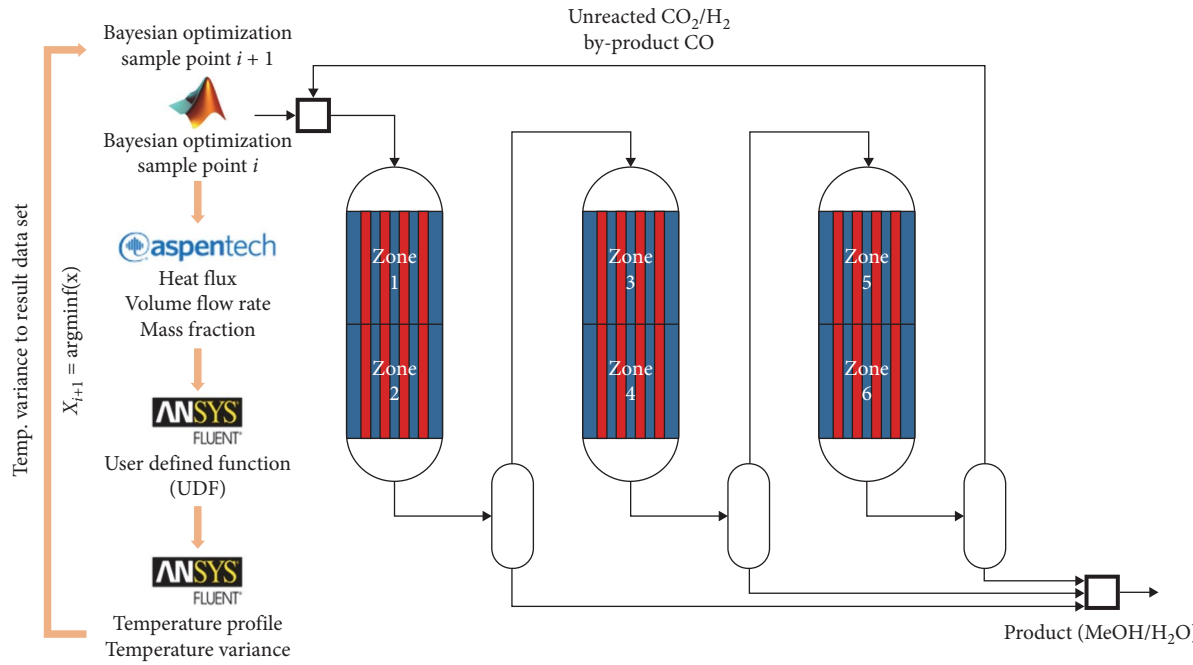


FIGURE 2: Schematic representation of the shortcut optimization platform for direct CO_2 hydrogenation. The platform integrates a low-dimensional process model with a high-dimensional CFD model to enhance computational efficiency. A GPBO framework is employed to reduce the number of iterations and minimize the reliance on CFD simulations.

2.2. Integration of CFD Simulation With Process Model. Previous studies on multitubular reactor systems for methanol production primarily focused on conceptual process design using process simulators, without detailed consideration of the temperature profile within the reactor through CFD analysis [10, 11]. Performing process optimization with rigorous CFD simulation is highly challenging due to the long computation time required for a single CFD run and the large number of iterations needed for optimization. Therefore, this study developed a shortcut platform for efficient CFD-based optimization of the direct CO_2 hydrogenation system, aided by a process model, as shown in Figure 2. This platform consists of two levels: a low dimensional process model and a high dimensional CFD model. The CFD model is integrated with the process model to reduce the computational burden at each iteration. In addition, an efficient optimization algorithm (GPBO) was employed to minimize the number of iterations and identify the optimal solution with fewer CFD simulations [41].

CFD tools solve transport phenomena for a given geometry using finite volume methods. In reactor simulations, Arrhenius-type reaction kinetics are typically applied to each finite volume. However, the direct CO_2 hydrogenation process studied here is a heterogeneous reaction, where gas molecules adsorb onto the solid catalyst surface and react. To accurately model this behavior, Langmuir–Hinshelwood-type reaction kinetics were implemented through user-defined functions (UDFs). Due to the highly nonlinear nature of Langmuir–Hinshelwood equations, incorporating these reaction kinetics significantly increases the complexity of CFD simulations, making it more challenging to obtain an optimal solution within a feasible computation time.

In this framework, the process simulator exclusively calculates key process variables, including heat duty, volumetric flow rate, and mass fractions. Among these, heat duty and volumetric flow rate were converted into heat flux (Equation (4)) and inlet velocity (Equation (5)), respectively. The process simulation data was imported into the CFD tool through UDFs. Inlet velocity and mass fractions from the process simulation were applied as boundary conditions in the CFD simulation for mass balance and fluid dynamics calculations. Heat flux, on the other hand, represented the volumetric heat sources (S_h in Equation (6)) in the energy balance, accounting for the heat generated by reactions inside the reactors. The CFD tool then computed the temperature distribution for each finite volume.

$$\text{Heat flux}\left(\text{W/m}^3\right) = \frac{\text{Heat duty (W)}}{\text{Number of tubes} \times \text{compartment volume}\left(\text{m}^3\right)}, \tag{4}$$

$$\text{Inlet velocity}\left(\text{m/s}\right) = \frac{\text{Volume flow rate}\left(\text{m}^3/\text{s}\right)}{\text{Number of tubes} \times \text{inlet area}\left(\text{m}^2\right)}, \tag{5}$$

$$\frac{\partial}{\partial t}(\rho \text{E}) + \nabla \cdot (\vec{\nu}(\rho E + p)) = \nabla \cdot \left(k_{eff} \nabla T - \sum_j h_j \vec{J}_j + \left(\overline{\overline{\tau}}_{eff} \cdot \vec{\nu}\right)\right) + S_h. \tag{6}$$

The shortcut platform developed in this study was operated within a Matlab R2019b modeling environment. Integration

ijer, 2025, 1, Downloaded from https://onlinelibrary.wiley.com/doi/10.1155/er/2329142 by Ewha Womans University Library, Wiley Online Library on [20/05/2026]. See the Terms and Conditions (https://onlinelibrary.wiley.com/terms-and-conditions) on Wiley Online Library for rules of use; OA articles are governed by the applicable Creative Commons License

between the CFD model in Ansys Fluent V19.2 and the process model in Aspen Plus V10 was achieved through the GPBO algorithm implemented in Matlab. First, Matlab communicated with Aspen Plus using Component Object Model (COM) technology. Through the COM interface, Matlab updated the catalyst loading values determined by the GPBO, executed Aspen Plus simulations, and retrieved the simulation results. Based on these process simulation results, Matlab then generated the necessary input files for the CFD simulation, including a text-based user interface (TUI) journal file containing all required Ansys Fluent commands and a UDF written in C++. Using the TUI file, Matlab launched Ansys Fluent to perform the CFD simulation and subsequently extracted the resulting temperature profiles. Further details are provided in the supporting information (Table S1).

2.3. Optimization Formulation. The objective of the optimizations in this study was to minimize the temperature difference within the methanol reactors by adjusting catalyst loadings, while maintaining key reaction performance metrics such as methanol yield, purity, and the total catalyst amount. Several indices can be used to evaluate a reactor's temperature profile, including the maximum temperature gap and the variance of the temperature distribution. In this study, the minimization of temperature variance along the axial direction was selected as the objective function. In Equations (7) and (8), i and j denote the reactor number and the internal point index within a reactor, respectively. A total of three reactors were considered, each containing 401 internal points, as finite volumes with an axial resolution of 1 cm were assumed.

$$\min \sum_i \mathrm{Var}_i, \tag{7}$$

$$\mathrm{Var}_i = \frac{\sum_j \left(T_{\mathrm{i},j} - T_{i,\mathrm{avg}}\right)^2}{n}, \tag{8}$$

The model adjusted the catalyst loadings in each zone to achieve an optimal temperature profile while maintaining the total catalyst amount at 865 kg [10, 11]. The product yield and purity at the optimal conditions were required to be at least 12,500 kg/h and 99.9%, respectively. In Equations (9)–(11), k represents the number of reaction zones, w denotes the catalyst weight (kg), m corresponds to the product yield (kg/h), and f represents the product purity. An optimization algorithm distributed the total 865 kg of catalyst across six zones, and a process simulator verified these inequality constraints using the "design specs" function.

$$\sum_k w_k = 865, \tag{9}$$

$$m_{\mathrm{methanol}} \geq 12,500, \tag{10}$$

$$f_{\mathrm{methanol}} \geq 0.999. \tag{11}$$

2.4. Learning-Based Optimization. In addition to the shortcut modeling platform designed to reduce simulation time, a learning-based optimization approach was employed to optimize catalyst loading and the temperature profile in the direct CO_2 hydrogenation reactor system. This approach aimed to minimize the number of simulations required during optimization runs. The GPBO algorithm used in this study is highly efficient for black-box model optimization. Compared to other optimization algorithms, GPBO requires significantly fewer function evaluations to reach the optimum, thereby reducing computational time.

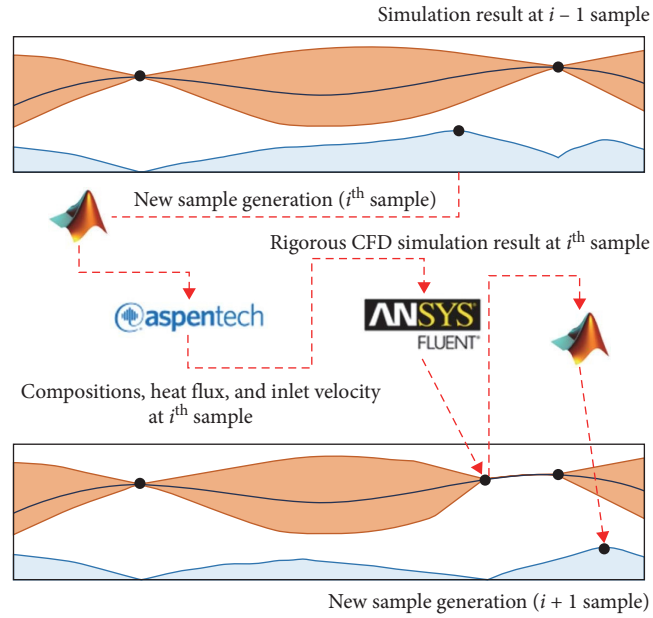


FIGURE 3: Schematic representation of the GPBO framework for catalyst loading and temperature profile optimization. The optimization loop integrates Matlab for optimization, Aspen Plus for process simulations, and Ansys Fluent for CFD analysis. The iterative process updates the Gaussian process surrogate model, which balances exploration and exploitation to minimize the number of simulations required for optimization.

GPBO operates by constructing a probabilistic surrogate model of the objective function using Gaussian processes. This surrogate model provides a predictive mean and variance at unexplored points, allowing the algorithm to estimate not only the function value but also its uncertainty. Based on this information, an acquisition function is used to determine the next sample point by balancing exploration (sampling in uncertain regions) and exploitation (sampling near the estimated optimum). By leveraging this probabilistic framework, GPBO efficiently navigates complex, high-dimensional search spaces while mitigating the risk of local optima. Figure 3 illustrates the GPBO framework integrated with CFD and process models. In Matlab, Gaussian process surrogate models were established to represent the input–output relationships of the black-box optimization model. These surrogate models were iteratively refined using sampled data from previous simulations. The selection of the next sample point was guided by a balance between exploitation and exploration. Thompson sampling was used to manage this trade-off effectively. The simulation at the selected sample point was performed using Aspen Plus for

ijer, 2025, 1, Downloaded from https://onlinelibrary.wiley.com/doi/10.1155/er/2329142 by Ewha Womans University Library, Wiley Online Library on [20/05/2026]. See the Terms and Conditions (https://onlinelibrary.wiley.com/terms-and-conditions) on Wiley Online Library for rules of use; OA articles are governed by the applicable Creative Commons License

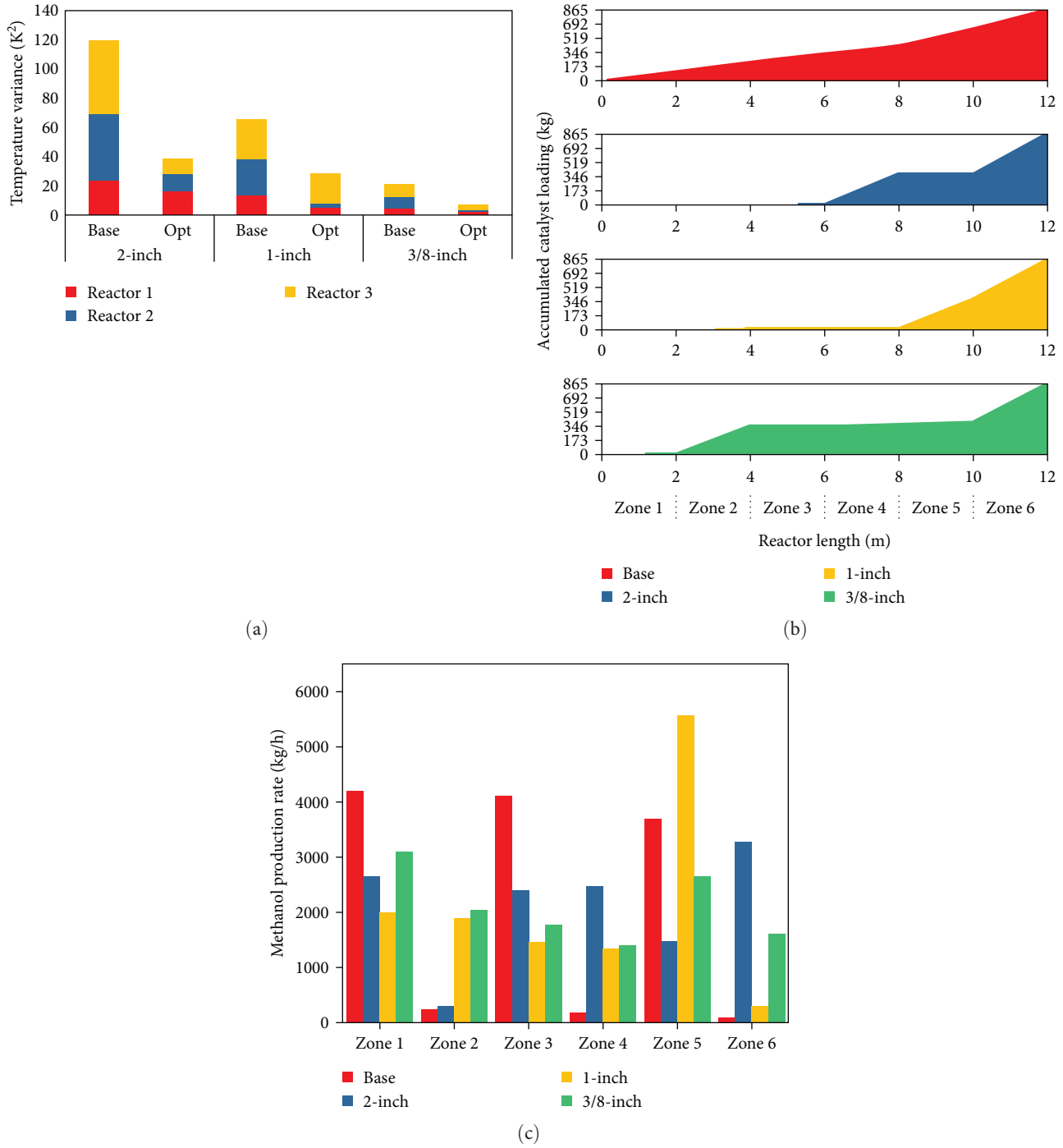


FIGURE 4: (a) Temperature variance comparison between base and optimized cases, showing over 50% reduction across all tube sizes. The reduced variance indicates improved thermal management and enhanced operational safety by mitigating hot spot formation. (b) Optimized catalyst loading distributions across six reactor zones, revealing uneven but strategically adjusted catalyst packing that promotes more uniform reaction heat generation. (c) Methanol production rates, demonstrating improved reaction distribution and more effective catalyst utilization in the optimized cases, which contribute to greater reactor efficiency and longer catalyst lifetime.

the process model and Ansys Fluent for the CFD model. The resulting simulation data were then fed back into Matlab to update the surrogate models, continuing the iterative optimization process.

3. Results and Discussion

The optimization was conducted on a system equipped with a Ryzen 3700x CPU (8 cores, 16 threads) and 16 GB of RAM.

ijer, 2025, 1, Downloaded from https://onlinelibrary.wiley.com/doi/10.1155/er/2329142 by Ewha Womans University Library, Wiley Online Library on [20/05/2026]. See the Terms and Conditions (https://onlinelibrary.wiley.com/terms-and-conditions) on Wiley Online Library for rules of use; OA articles are governed by the applicable Creative Commons License

Using the conventional CFD approach, which implements Langmuir–Hinshelwood reaction kinetics via a UDF, a single simulation point typically requires over 15 min of computation time. As a result, the total optimization process may take more than 2 weeks, rendering it impractical for reactor design applications. In contrast, the proposed platform—integrating Matlab, Aspen Plus, and Ansys Fluent—reduces the computation time per point to under 3 min, accelerating the overall optimization process by more than a factor of five. In conventional methods, the UDF approach necessitates a time step size of 10^{-6} s or smaller due to the inherently fast initial reaction rate of the CO_2-to-methanol conversion. Larger time steps fail to capture both the forward and reverse reactions accurately, leading to numerical divergence and a lack of convergence. However, in the proposed framework, reaction kinetics are computed through a subroutine, avoiding excessive computational demands. This approach achieves the same level of accuracy while maintaining the significantly reduced computation time of under 3 min per iteration.

The optimization of the temperature profile for a multistage methanol reactor system was performed using GPBO, implemented in Matlab and coupled with Aspen Plus and Ansys Fluent. GPBO is a probabilistic machine-learning approach that iteratively improves a surrogate model of the reactor's behavior, significantly reducing the number of required simulations compared to conventional optimization techniques. Unlike gradient-based optimizers, GPBO does not require an explicit mathematical model of the objective or continuous differentiability. It treats the reactor as a "black box" and can handle multiple operating parameters simultaneously, avoiding local optima by balancing exploration and exploitation. The convergence of the GPBO for each reactor size is shown in Figure S1, which indicates faster convergence with increasing tube diameter. The mass and energy balances for the 2-inch tubular reactor case, based on Figure 1, are also provided in Table S2.

Figure 4 compares temperature variance, optimized catalyst loading distributions, and methanol production rates, highlighting the more uniform temperature profiles and improved reaction distribution in the optimized cases. Figure 4a illustrates the optimized objective function values, showing reductions of over 50% in overall temperature variance for all three tube sizes. In the optimized cases, temperature fluctuations were significantly reduced, with the largest improvements observed in the 2-inch tube configurations. These reductions indicate that GPBO effectively minimized temperature fluctuations, enhancing thermal stability, prolonging catalyst lifetime, and improving methanol yield. This result is particularly important because excessive temperature variations can shift reaction equilibria unfavorably, accelerate catalyst deactivation, and reduce overall methanol productivity.

The primary mechanism behind the reduction in temperature variance was the nonuniform distribution of catalyst loading, which enabled better control of the methanol synthesis rate. Figure 4b presents the optimized catalyst loading distribution, while Figure 4c shows the corresponding methanol production rates across different reactor zones. In the base case, with uniformly distributed catalyst, methanol synthesis occurred predominantly near the reactor inlet due to high reactant concentrations and fast reaction kinetics. However, the high exothermicity of methanol synthesis led to an intense hot spot near the reactor entrance, causing rapid temperature rise. These high temperatures could reduce net methanol production and result in inefficient catalyst utilization. Furthermore, in the latter half of the reactor, where reactant concentrations were lower, reaction rates slowed considerably, leading to underutilization of the catalyst. For example, in reactor 2 of the base case, the methanol mass fraction increased from 0.8% to 14.2% in the first half of the reactor but only from 14.2% to 14.8% in the second half, highlighting the severe imbalance in reaction activity. Similarly, zones 2, 4, and 6 of all reactors exhibited poor reaction performance in the base case.

In contrast, the optimized case showed a more even reaction distribution along the reactor length. By reducing catalyst loading near the inlet, heat release was moderated, preventing excessive temperature rises. At the same time, increasing catalyst loading in later reaction zones compensated for lower reactant concentrations, allowing the reaction to proceed more effectively throughout the reactor. This adjustment flattened the temperature profile and maintained a higher methanol yield over the entire reactor length. The methanol mass fraction increased more evenly, rising from 0.9% to 7.1% in the first half and from 7.1% to 13.4% in the second half, demonstrating the effectiveness of this redistribution strategy.

In contrast, the optimized case exhibited a more even reaction distribution along the reactor length. By reducing catalyst loading near the inlet, heat release was moderated, preventing excessive temperature rises. Simultaneously, increasing catalyst loading in the later reaction zones compensated for lower reactant concentrations, allowing reactions to proceed more effectively throughout the reactor. This adjustment flattened the temperature profile and maintained higher methanol yield across the reactor length. The methanol mass fraction increased more evenly, rising from 0.9% to 7.1% in the first half and from 7.1% to 13.4% in the second half, demonstrating the effectiveness of this redistribution strategy.

These improvements are clearly visualized in the temperature profiles. In the base case, all reactors exhibit intense, localized heat release at the inlet. This is particularly pronounced in reactor 1 across all tube sizes, where the base case shows steep peaks in the first 0.5–0.7 m, indicative of concentrated exothermic activity. In contrast, the optimized cases show a flattened and extended heat flux profile. In reactor 2, the base case still displays inlet-dominated heat release, while the optimized case introduces a distinct secondary peak downstream, evidencing reactivated catalyst zones later in the reactor. Reactor 3 in the base case shows limited heat release, indicating depleted reactants. However, in the optimized case, a secondary heat flux peak emerges mid-reactor, suggesting that catalyst in this zone was effectively re-engaged to enhance conversion. The trend is most

ijer, 2025, 1, Downloaded from https://onlinelibrary.wiley.com/doi/10.1155/er/2329142 by Ewha Womans University Library, Wiley Online Library on [20/05/2026]. See the Terms and Conditions (https://onlinelibrary.wiley.com/terms-and-conditions) on Wiley Online Library for rules of use; OA articles are governed by the applicable Creative Commons License

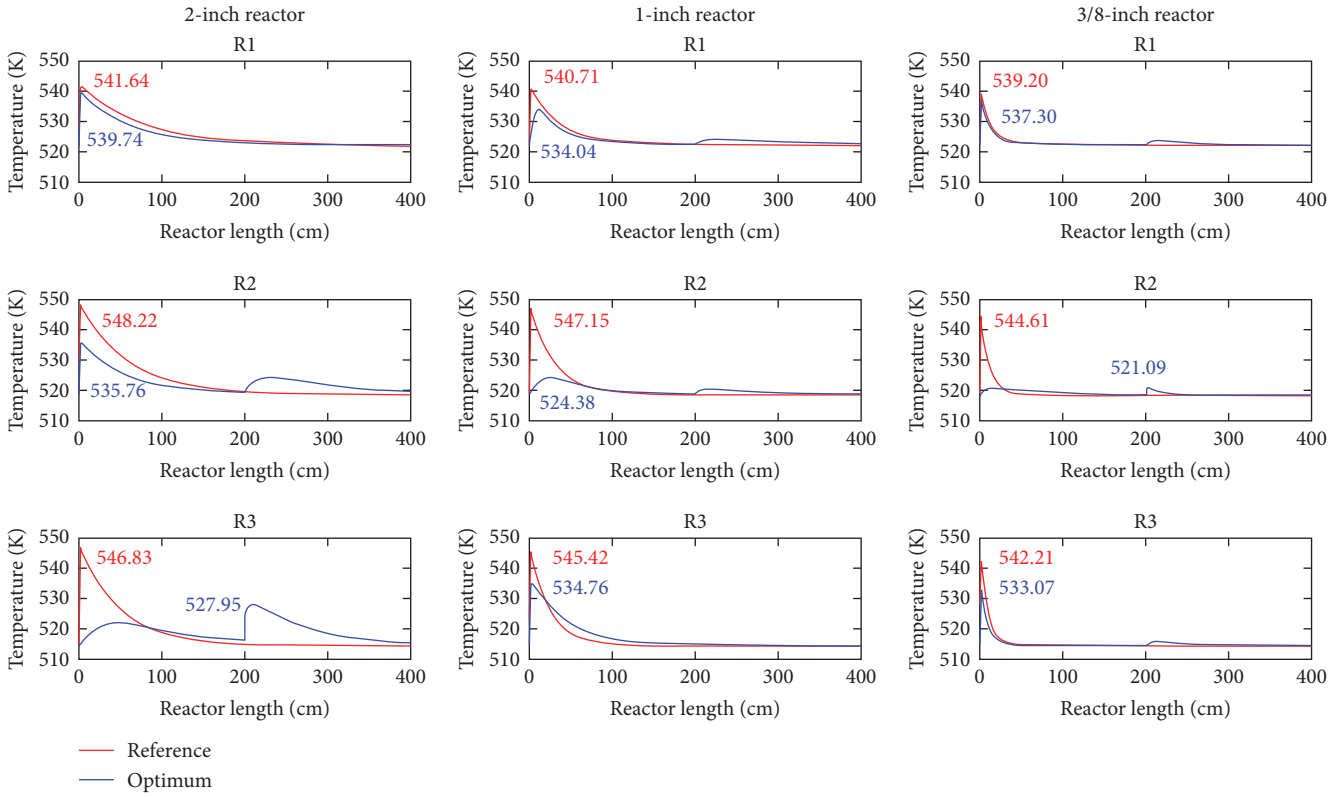


FIGURE 5: Axial temperature profiles for all reactors and tube sizes. Optimized cases exhibit markedly reduced inlet hot spots and more uniform temperature distributions across the reactor length, reflecting improved heat removal and enhanced thermal control. The more gradual temperature rise also reactivates downstream catalytic zones, leading to higher overall catalyst utilization and greater operational stability. These trends are consistent with the quantitative results summarized in Table S3, where both axial and radial temperature differences were significantly reduced.

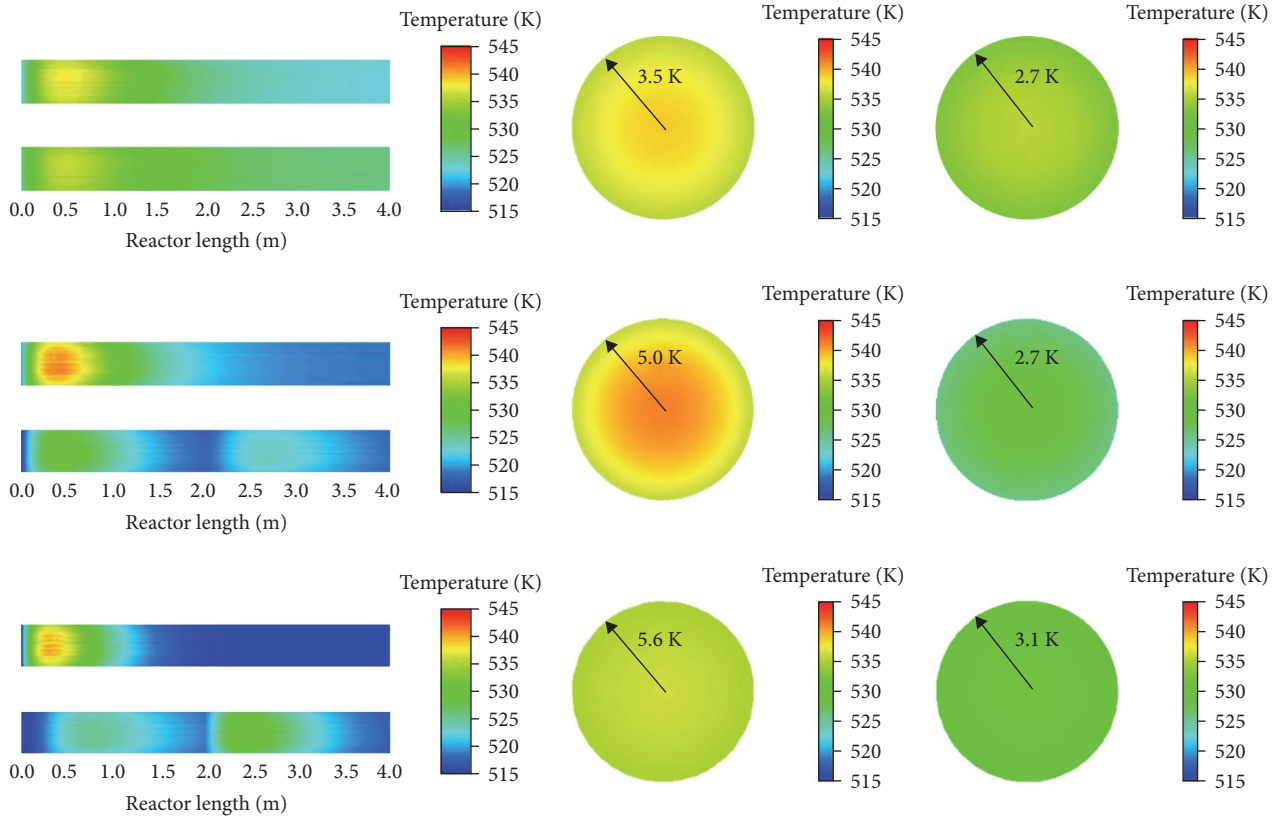
pronounced in the 3/8-inch tubes, where superior radial heat transfer enables high-intensity but well-controlled reaction zones throughout the reactor.

The temperature profiles in Figure 5 illustrate these observations. In the base case, reactor 1 exhibits a rapid temperature rise near the inlet, particularly in the 2-inch tubes, where the peak temperature reaches approximately 550 K. In contrast, the optimized profiles show a smoother and more gradual increase, with the peak temperature reduced by more than 10 K, reaching 535.76 K. In reactor 2, the base case displays a steep temperature drop following the inlet hot spot, whereas the optimized case maintains a more stable profile with a secondary temperature rise downstream. This behavior indicates that heat release and reaction activity were effectively redistributed through catalyst reallocation. In reactor 3, the temperature in the base case declines steadily, reflecting an inactive final stage. However, in the optimized case, the temperature profile exhibits a rise in the mid-to-late section, confirming improved catalyst engagement and enhanced thermal balance. Across all tube sizes, the optimized profiles exhibit less steep gradients and more uniform temperatures, which is critical for maintaining catalyst stability and prolonging reactor performance.

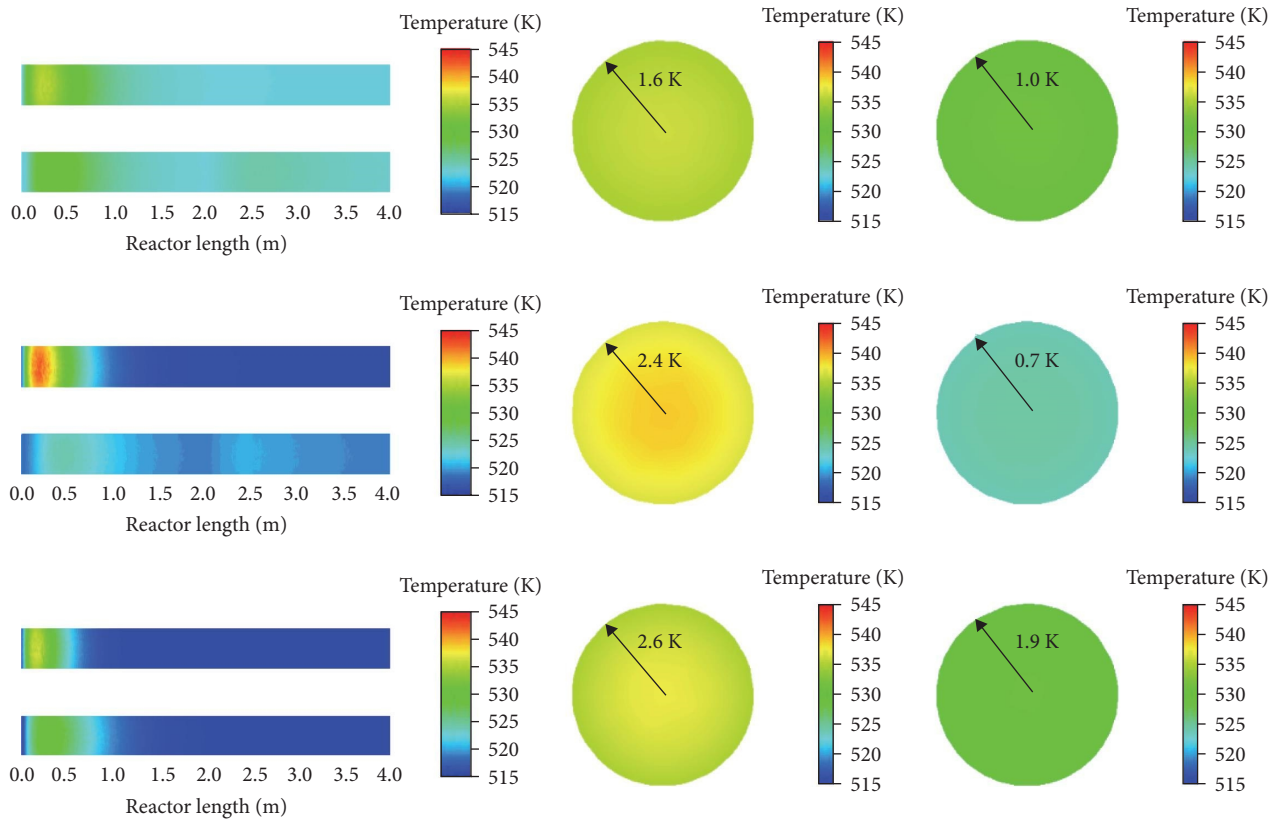
The effect of tube size on thermal performance is also critical. The 3/8-inch tube configuration consistently showed the lowest temperature variance across all reactors due to its high surface-to-volume ratio and shorter radial heat transfer distance. This facilitated more effective removal of reaction heat, providing better control over temperature rise and hot spot formation, as shown in Figure 6 and Table S3. Smaller tubes are, therefore, favorable from the perspective of temperature control. However, in practice, multiple factors must be considered, including cost, operability, maintenance, selectivity, and catalyst deactivation. A more uniform temperature distribution enhances operability by stabilizing temperature-dependent selectivity and reducing catalyst deactivation; however, achieving this requires smaller tube sizes and a substantially larger number of tubes (3240 in the 1-inch system vs. 23,040 in the 3/8-inch system), which complicates maintenance and increases cost. The estimated equipment costs for the 2-, 1-, and 3/8-inch tube reactors in Table S4 are 36.6, 37.1, and 49.3 million USD, respectively.

When balancing thermal performance and cost, the 1-inch tube system represents the most practical compromise relative to the 3/8-inch system. Under the optimal conditions, the maximum radial temperature differences were 1.9 K for the 1-inch tubes and 1.0 K for the 3/8-inch tubes. Specifically, the 1-inch tube system achieved a 38.7% reduction in maximum radial temperature difference compared with the 2-inch system (3.1 K), with only a 1.4% increase in capital investment. In contrast, the 3/8-inch tube system achieved a 67.7% reduction but required a 34.7% increase in

ijer, 2025, 1, Downloaded from https://onlinelibrary.wiley.com/doi/10.1155/er/2329142 by Ewha Womans University Library, Wiley Online Library on [20/05/2026]. See the Terms and Conditions (https://onlinelibrary.wiley.com/terms-and-conditions) on Wiley Online Library for rules of use; OA articles are governed by the applicable Creative Commons License



(a)



(b)

Figure 6: Continued.

ijer, 2025, 1, Downloaded from https://onlinelibrary.wiley.com/doi/10.1155/er/2329142 by Ewha Womans University Library, Wiley Online Library on [20/05/2026]. See the Terms and Conditions (https://onlinelibrary.wiley.com/terms-and-conditions) on Wiley Online Library for rules of use; OA articles are governed by the applicable Creative Commons License

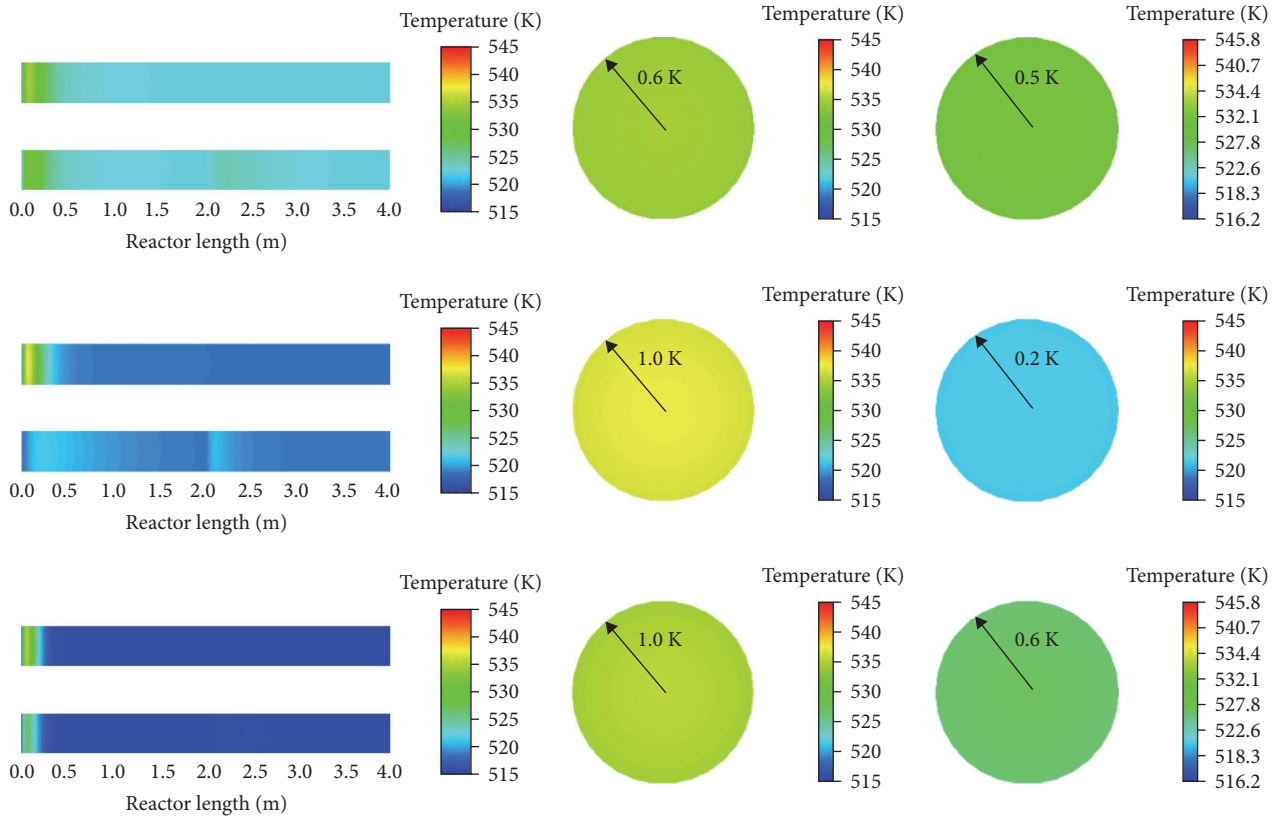


FIGURE 6: Axial and cross-sectional temperature profiles at reactor hot spots for (a) 2-inch, (b) 1-inch, and (c) 3/8-inch tubes. The optimized cases exhibit substantially reduced axial and radial temperature gradients, confirming enhanced heat management and effective suppression of localized hot spots. These improvements contribute to safer operation, lower thermal stress on reactor materials, and extended catalyst lifetime. The quantitative reductions in temperature differences are summarized in Table S3.

capital investment relative to the 2-inch system. Therefore, the 1-inch tube reactor can be considered the most practical choice.

The optimization results obtained in this study are noteworthy. Cui and Kær [9] conducted a CFD-based case study comparing temperature distributions in different reactor types (adiabatic, gas-cooled, and water-cooled) under various operating conditions, including feed composition, inlet temperature, and pressure. They concluded that the water-cooled reactor outperformed the others; however, their results still showed considerable temperature variations—approximately 25–65 K axially and 4–15 K radially in 40 mm multitubular reactors. In contrast, the present study performed a full optimization, rather than a case study, achieving markedly improved temperature uniformity, with axial and radial temperature differences reduced to 14.6 and 3.1 K, respectively, in 2-inch (51 mm) tubes.

The effect of CO in the feed on the temperature profile was also investigated. In the direct CO_2 hydrogenation process for methanol synthesis studied here, the recycle stream contained CO produced via the RWGS reaction, in addition to unreacted CO_2 and H_2. Consequently, all reactor inlet streams contained CO, which can convert to methanol with a larger amount of reaction heat (−90.77 kJ/mol, Equation (3)) than that for CO_2-to-methanol (−49.16 kJ/mol, Equation (1)). As a result, the presence of CO in the feed complicates thermal control in the methanol reactors. Figure S2 compares the temperature profiles with and without CO in the feed by adding or removing the recycle stream in the base case. The results show a more rapid temperature rise with CO: an axial increase of 19.4 K with CO versus 10.1 K without CO. This behavior can be attributed to the promotional effect of CO on CTM, as reported in the literature. DFT calculations have demonstrated the accelerating effect of CO on the direct CO_2 hydrogenation steps [42, 43], which has also been confirmed by several experimental studies [44].

4. Conclusions

In this study, a shortcut modeling platform was developed and applied to a multitubular reactor system for methanol synthesis via direct CO_2 hydrogenation. The platform enabled complex optimization that would otherwise require numerous iterations with high computational cost due to the large size of the modeling problem and the highly nonlinear reaction kinetics. Instead of performing a full CFD simulation at each iteration, the platform utilized a process simulator to describe the reactions in the reactors, thereby significantly reducing the computational burden. Based on the process simulation results, CFD simulations were subsequently

ijer, 2025, 1, Downloaded from https://onlinelibrary.wiley.com/doi/10.1155/er/2329142 by Ewha Womans University Library, Wiley Online Library on [20/05/2026]. See the Terms and Conditions (https://onlinelibrary.wiley.com/terms-and-conditions) on Wiley Online Library for rules of use; OA articles are governed by the applicable Creative Commons License

conducted to investigate the internal temperature profiles of the reactors. A machine-learning-based optimization algorithm (GPBO) was employed to identify optimal solutions with fewer iterations. The entire optimization process was implemented in the Matlab environment, integrated with Aspen Plus and Ansys Fluent.

The platform was applied to a three-tubular-reactor system for CTM. The exothermic nature of methanol synthesis caused unfavorable temperature profiles in the reactors. Therefore, the platform was used to minimize temperature variance by employing uneven catalyst loading in the reactors. The optimized uneven catalyst loading caused more evenly distributed heat generation, resulting in significantly more uniform temperature profiles. The optimization reduced temperature variance by 67.5% for 2-inch tubes, 55.4% for 1-inch tubes, and 67.3% for 3/8-inch tubes. The maximum axial temperature differences were substantially reduced, for example, in reactor 2 with 3/8-inch tubes, from 18.8 to 3.1 K (a reduction of 15.7 K). In the radial direction, the hot spot in reactor 3 with 2-inch tubes decreased by 2.5, from 5.6 to 3.1 K.

The effect of CO in the feed was also investigated, as CO is an intermediate and a well-known promoter of the CO_2 hydrogenation reaction. CO, produced via the RWGS reaction in the reactors, was reintroduced to the feed through the recycle system. Due to its promotional effect, the maximum temperature difference in a tubular reactor increased from 10.1 to 19.4 K.

Overall, the results of this study provide valuable insights for the design and optimization of not only multitubular reactors but also other reactor types. The findings from different tube diameters allow prediction of efficiency loss during scale-up. Furthermore, the proposed shortcut modeling platform enhances reactor operation by maintaining uniform temperature profiles, thereby improving stability and controllability. It also increases safety by preventing thermal runaway and improves economic performance by lowering hot spot temperatures and mitigating catalyst deactivation. Because this methodology involves only adjusting catalyst loadings, it can be readily applied to existing reactors for revamping, leading to improved overall performance.

Data Availability Statement

The data that support the findings of this study are available from the corresponding author upon reasonable request.

Conflicts of Interest

The authors declare no conflicts of interest.

Funding

This study was funded by the Korea Institute of Science and Technology, Ministry of Science and ICT, South Korea (Grants NRF-2022M3C1A3092056 and RS-2023-00259920) and the Korea Institute of Energy Technology Evaluation and Planning, (Grant 20225A10100090).

Acknowledgments

This work was supported by the Methanol Project (20225A10100090) through the Korea Institute of Energy Technology Evaluation and Planning (KETEP) (Ministry of Trade, Industry and Energy, Republic of Korea) and NRF-2022M3C1A3092056 and RS-2023-00259920 through the National Research Foundation (NRF) funded by the Ministry of Science and ICT, Republic of Korea. The authors acknowledge the support from Korea Institute of Science and Technology (KIST) institutional program.

Supporting Information

Additional supporting information can be found online in the Supporting Information section. (*Supporting Information*) Table S1. Simulation settings for the shortcut platform. Table S2. Heat and material balance sheet for the optimal result. Table S3. Maximum temperature differences of the reactors in the axial and radial directions. Table S4. Equipment cost. Figure S1. Convergence rate of the reactor model integrating Matlab, Aspen Plus, and Ansys Fluent platform. Optimization was performed using the GPBO algorithm. Figure S2. Effect of CO in feed on temperature profile: (a) CO flow rate and (b) temperature profile.

References

[1] International Energy Agency, "Energy Technology Perspectives," (2020).

[2] E. Alper and O. Y. Orhan, "CO2 Utilization: Developments in Conversion Processes," *Petroleum* 3, no. 1 (2017): 109–126.

[3] T. A. Atsbha, T. Yoon, P. Seongho, and C.-J. Lee, "A Review on the Catalytic Conversion of CO_2 Using H2 for Synthesis of CO, Methanol, and Hydrocarbons," *Journal of CO_2 Utilization* 44 (2021): 101413.

[4] X. Dong, S. Ma, and P. Gao, "The Development of Uncalcined Cu-Based Catalysts by Liquid Reduction Method for CO_2 Hydrogenation to Methanol," *Catalysis Letters* 153, no. 6 (2023): 1696–1707.

[5] Z. Xie, J. Hei, L. Cheng, J. Li, X. Yin, and S. Meng, "Influence of Cu/Al Ratio on the Performance of Carbon-Supported Cu/ZnO/Al2O3 Catalysts for CO2 Hydrogenation to Methanol," *Catalysts* 13, no. 5 (2023): 800.

[6] E. B. Agyekum, P. C. Okonkwo, and F. L. Rashid, "Research on Biomass Energy and CO2 Conversion to Methanol: A Combination of Conventional and Bibliometric Review Analysis," *Carbon Research* 4, no. 1 (2025): 4.

[7] S. Mbatha, R. C. Everson, N. M. Musyoka, H. W. Langmi, A. Lanzini, and W. Brilman, "Power-to-Methanol Process: A Review of Electrolysis, Methanol Catalysts, Kinetics, Reactor Designs and Modelling, Process Integration, Optimisation, and Techno-Economics," *Sustainable Energy & Fuels* 5, no. 14 (2021): 3490–3569.

[8] M. E. Sarvestani, O. Norouzi, F. Di Maria, and A. Dutta, "From Catalyst Development to Reactor Design: A Comprehensive Review of Methanol Synthesis Techniques," *Energy Conversion and Management* 302 (2024): 118070.

[9] X. Cui and S. K. Kær, "A Comparative Study on Three Reactor Types for Methanol Synthesis From Syngas and CO_2," *Chemical Engineering Journal* 393 (2020): 124632.

ijer, 2025, 1, Downloaded from https://onlinelibrary.wiley.com/doi/10.1155/er/2329142 by Ewha Womans University Library, Wiley Online Library on [20/05/2026]. See the Terms and Conditions (https://onlinelibrary.wiley.com/terms-and-conditions) on Wiley Online Library for rules of use; OA articles are governed by the applicable Creative Commons License

[10] A. A. Kiss, J. Pragt, H. Vos, G. Bargeman, and M. T. De Groot, "Novel Efficient Process for Methanol Synthesis by CO2 Hydrogenation," *Chemical Engineering Journal* 284 (2016): 260–269.

[11] H. W. Lee, K. Kim, J. An, et al., "Toward the Practical Application of Direct CO_2 Hydrogenation Technology for Methanol Production," *International Journal of Energy Research* 44, no. 11 (2020): 8781–8798.

[12] A. Mirvakili, S. Chahibakhsh, M. Ebrahimzadehsarvestani, E. Soroush, and M. Rahimpour, "Modeling and Assessment of Novel Configurations to Enhance Methanol Production in Industrial Mega-Methanol Synthesis Plant," *Journal of the Taiwan Institute of Chemical Engineers* 104 (2019): 40–53.

[13] A. Keshavarz, A. Mirvakili, S. Chahibakhsh, A. Shariati, and M. Rahimpour, "Simultaneous Methanol Production and Separation in the Methanol Synthesis Reactor to Increase Methanol Production," *Chemical Engineering and Processing - Process Intensification* 158 (2020): 108176.

[14] A. Mirvakili and M. Rahimpour, "Mal-Distribution of Temperature in an Industrial Dual-Bed Reactor for Conversion of CO_2 to Methanol," *Applied Thermal Engineering* 91 (2015): 1059–1070.

[15] F. Samimi, M. Feilizadeh, M. Ranjbaran, M. Arjmand, and M. R. Rahimpour, "Phase Stability Analysis on Green Methanol Synthesis Process From CO2 Hydrogenation in Water Cooled, Gas Cooled and Double Cooled Tubular Reactors," *Fuel Processing Technology* 181 (2018): 375–387.

[16] A. Mirvakili, A. Bakhtyari, and M. R. Rahimpour, "A CFD Modeling to Investigate the Impact of Flow Mal-Distribution on the Performance of Industrial Methanol Synthesis Reactor," *Applied Thermal Engineering* 128 (2018): 64–78.

[17] L. Zhang, W. Yu, X. Pan, et al., "Thermal Hazard Assessment for Synthesis of 3-Methylpyridine-N-Oxide," *Journal of Loss Prevention in the Process Industries* 35 (2015): 316–320.

[18] R. Henda, A. Machac, and B. Nilsson, "Heat and Mass Transport in a Nonlinear Fixed-Bed Catalytic Reactor: Hot Spots and Thermal Runaway," *Chemical Engineering Journal* 143, no. 1–3 (2008): 195–200.

[19] V. Barrio, G. Schaub, M. Rohde, et al., "Reactor Modeling to Simulate Catalytic Partial Oxidation and Steam Reforming of Methane. Comparison of Temperature Profiles and Strategies for Hot Spot Minimization," *International Journal of Hydrogen Energy* 32, no. 10-11 (2007): 1421–1428.

[20] Q. Chen, J. Wang, M. Gao, L. Liu, and J. Tao, "Review on Loss Prevention of Chemical Reaction Thermal Runaway: Principles and Application," *Emergency Management Science and Technology* 2, no. 1 (2022): 1–8.

[21] R. Agrawal, D. H. West, and V. Balakotaiah, "Modeling and Analysis of Local Hot Spot Formation in Down-Flow Adiabatic Packed-Bed Reactors," *Chemical Engineering Science* 62, no. 18–20 (2007): 4926–4943.

[22] A. Montebelli, C. G. Visconti, G. Groppi, E. Tronconi, and S. Kohler, "Optimization of Compact Multitubular Fixed-Bed Reactors for the Methanol Synthesis Loaded With Highly Conductive Structured Catalysts," *Chemical Engineering Journal* 255 (2014): 257–265.

[23] I. Nájera, J. Álvarez, R. Baratti, and C. Gutiérrez, "Control of an Exothermic Packed-Bed Tubular Reactor," *IFAC-PapersOnLine* 49, no. 7 (2016): 278–283.

[24] W. Jung, S.-H. Shin, S. Park, et al., "Unveiling Key Descriptors of Ionomer Materials for Enhanced Electrochemical CO_2 Reduction," *ACS Energy Letters* 10, no. 1 (2025): 620–628.

[25] S. H. Yang, W. Jung, H. Lee, et al., "Membrane Engineering Reveals Descriptors of CO_2 Electroreduction in an Electrolyzer," *ACS Energy Letters* 8, no. 4 (2023): 1976–1984.

[26] D. Kim, W. Choi, H. W. Lee, et al., "Electrocatalytic Reduction of Low Concentrations of CO2 Gas in a Membrane Electrode Assembly Electrolyzer," *ACS Energy Letters* 6, no. 10 (2021): 3488–3495.

[27] A. Sari and J. Sabziani, "Modeling and 3D-Simulation of Hydrogen Production via Methanol Steam Reforming in Copper-Coated Channels of a Mini Reformer," *Journal of Power Sources* 352 (2017): 64–76.

[28] M. Ziarati, M. A. Ghafouri Roozbahani, and N. Khandan, "New Method of Rigorous Modeling and CFD Simulation for Methanol—Steam Reforming in Packed-Bed Reactors," *Chemical Engineering Communications* 203, no. 10 (2016): 1359–1373.

[29] K. S. Kshetrimayum, I. Jung, J. Na, et al., "Cfd Simulation of Microchannel Reactor Block for Fischer–Tropsch Synthesis: Effect of Coolant Type and Wall Boiling Condition on Reactor Temperature," *Industrial & Engineering Chemistry Research* 55, no. 3 (2016): 543–554.

[30] M. Irani, A. Alizadehdakhel, A. N. Pour, N. Hoseini, and M. Adinehnia, "CFD Modeling of Hydrogen Production Using Steam Reforming of Methane in Monolith Reactors: Surface or Volume-Base Reaction Model," 36, no. 24 (2011).

[31] R. E. Hayes and I. Cornejo, "Multi-Scale Modelling of Monolith Reactors: A 30-Year Perspective from 1990 to 2020," *The Canadian Journal of Chemical Engineering* 99, no. 12 (2021): 2589–2606.

[32] Z. Teimouri, V. B. Borugadda, A. K. Dalai, and N. Abatzoglou, "Application of Computational Fluid Dynamics for Modeling of Fischer-Tropsch Synthesis as a Sustainable Energy Resource in Different Reactor Configurations: A Review," *Renewable and Sustainable Energy Reviews* 160 (2022): 112287.

[33] F. Moradi, M. Kazemeini, and M. Fattahi, "A Three Dimensional CFD Simulation and Optimization of Direct DME Synthesis in a Fixed Bed Reactor," *Petroleum Science* 11, no. 2 (2014): 323–330.

[34] Y.-Q. Zhuang, X. Gao, Y.-P. Zhu, and Z.-H. Luo, "CFD Modeling of Methanol to Olefins Process in a Fixed-Bed Reactor," *Powder Technology* 221 (2012): 419–430.

[35] C. Kim, K. Park, H. Lee, et al., "Accelerating the Net-Zero Economy With CO2-Hydrogenated Formic Acid Production: Process Development and Pilot Plant Demonstration," *Joule* 8, no. 3 (2024): 693–713.

[36] J. Zhu, S. S. Araya, X. Cui, and S. K. Kær, "The Role of Effectiveness Factor on the Modeling of Methanol Steam Reforming over CuO/ZnO/Al2O3 Catalyst in a Multi-Tubular Reactor," *International Journal of Hydrogen Energy* 47, no. 14 (2022): 8700–8715.

[37] M. Son, Y. Woo, G. Kwak, Y.-J. Lee, and M.-J. Park, "CFD Modeling of a Compact Reactor for Methanol Synthesis: Maximizing Productivity With Increased Thermal Controllability," *International Journal of Heat and Mass Transfer* 145 (2019): 118776.

[38] J. Na, K. S. Kshetrimayum, U. Lee, and C. Han, "Multi-Objective Optimization of Microchannel Reactor for Fischer-Tropsch Synthesis Using Computational Fluid Dynamics and Genetic Algorithm," *Chemical Engineering Journal* 313 (2017): 1521–1534.

[39] J. Hwang, J. Kim, H. W. Lee, et al., "An Experimental Based Optimization of a Novel Water Lean Amine Solvent for Post

ijer, 2025, 1, Downloaded from https://onlinelibrary.wiley.com/doi/10.1155/er/2329142 by Ewha Womans University Library, Wiley Online Library on [20/05/2026]. See the Terms and Conditions (https://onlinelibrary.wiley.com/terms-and-conditions) on Wiley Online Library for rules of use; OA articles are governed by the applicable Creative Commons License

Combustion CO2 Capture Process," *Applied Energy* 248 (2019): 174–184.
[40] J. Im, S.-H. Cheong, H. T. Dang, et al., "Economically Viable Co-Production of Methanol and Sulfuric Acid via Direct Methane Oxidation," *Communications Chemistry* 6, no. 1 (2023): 282.
[41] U. Lee and A. Mitsos, "Optimal Multicomponent Working Fluid of Organic Rankine Cycle for Exergy Transfer From Liquefied Natural Gas Regasification," *Energy* 127 (2017): 489–501.
[42] L. Grabow and M. Mavrikakis, "Mechanism of Methanol Synthesis on Cu Through CO2 and CO Hydrogenation," *ACS Catalysis* 1, no. 4 (2011): 365–384.
[43] H.-W. Lim, M.-J. Park, S.-H. Kang, H.-J. Chae, J. W. Bae, and K.-W. Jun, "Modeling of the Kinetics for Methanol Synthesis Using Cu/ZnO/Al2O3/ZrO2 Catalyst: Influence of Carbon Dioxide During Hydrogenation," *Industrial & Engineering Chemistry Research* 48, no. 23 (2009): 10448–10455.
[44] O. Martin and J. Pérez-Ramírez, "New and Revisited Insights Into the Promotion of Methanol Synthesis Catalysts by CO2," *Catalysis Science & Technology* 3, no. 12 (2013): 3343–3352.

ijer, 2025, 1, Downloaded from https://onlinelibrary.wiley.com/doi/10.1155/er/2329142 by Ewha Womans University Library, Wiley Online Library on [20/05/2026]. See the Terms and Conditions (https://onlinelibrary.wiley.com/terms-and-conditions) on Wiley Online Library for rules of use; OA articles are governed by the applicable Creative Commons License